

The Influence of Piston Bowl Geometries on In-Cylinder Air Flow in a Direct-Injection (DI) Diesel Engine for Biodiesel Operation

S. Jaichandar

*Department of Automobile Engineering,
VelTech Dr RR & Dr SR Technical University,
Chennai, India
Email: jaisriram18@yahoo.com*

E. James Gunasekaran

*Department of Mechanical Engineering, Annamalai University,
Chidambaram, Tamil Nadu, India
Email: jamesgunasekaran@gmail.com*

A. Gunabalan

*Turbo Energy Private Limited, Chennai, India
Email: gunmit@gmail.com*

ABSTRACT

Thermal efficiency improvement, fuel consumption and pollutant emissions reduction from biodiesel fueled engines are critical requirements in engine research. In order to achieve these, a rapid and better air-fuel mixing condition is desired. The mixing quality of biodiesel with air can be improved by selecting the best engine design particularly combustion chamber design and injection system parameters. The present work investigates the effect of varying the piston bowl geometry on the air flow characteristics such as swirl velocity, Swirl Ratio (SR), and Turbulent Kinetic Energy (TKE) inside the engine cylinder. The piston's bowl geometry was modified into several configurations that include Shallow depth combustion chamber (SCC), Toroidal combustion chamber (TCC), Shallow depth reentrant combustion chamber (SRCC) and Toroidal re-entrant combustion chamber (TRCC) from the standard Hemispherical combustion chamber (HCC), without altering the compression ratio of the engine. A commercially available CFD code STAR-CD was used to analyze the in-cylinder flow at different conditions.

Flow conditions inside the cylinder were predicted by solving momentum, continuity and energy equations. The results confirmed that the piston bowl geometry had little influence on the in-cylinder flow during the intake stroke and the first part of compression stroke i.e. up to 300° after suction TDC. However, the piston bowl geometry plays a significant role in the latter stage of the compression stroke i.e. beyond 300° after suction TDC to compression TDC. The intensity of maximum swirl velocity at the end of compression stroke for TRCC was observed higher as 18.95 m/s and a strong recirculation was observed due to the geometry. Compared to baseline HCC the TRCC had higher, maximum swirl ratio and turbulent kinetic energy by about 28% and 2.14 times respectively. From the analysis of results, it was found that TRCC configuration gives better in-cylinder flows.

Keywords: *Diesel Engine, Combustion Chamber, Swirl Velocity, Swirl Ratio, Turbulent Kinetic Energy.*

Introduction

The main purpose of an internal combustion engine is to exhibit good performance while meeting the stringent emission standards. In order to meet those requirements, the outcomes of the combustion process are very important in internal combustion engines [1]. In-cylinder fluid dynamics in DI diesel engines plays a vital role for efficient combustion process [2]-[4]. It has been widely known that the engine performance and emissions of a compression ignition engine are dependent on the fuel vapour distribution in the cylinder. The efficiency of a DI diesel engine depends on the mixture preparation and its distribution inside the combustion chamber [5]. This phenomenon is based on the interaction of the in-cylinder air motion such as swirl, squish, tumble and turbulence and the spray characteristics from the high pressure injector. Hence, the shape of the combustion chamber geometry, the location of the injector, type of injector, air motion and fuel delivery characteristics become important factors for study [6].

The piston bowl geometry, location of injector, cylinder geometry and injection characteristics are important criteria in the design of DI diesel engines [2, 7]. The fuel evaporation and mixing processes are strongly influenced by the turbulent nature of the in-cylinder flows. In order to have better mixing, swirl is generated during the compression stroke as a result of combustion chamber geometry [8]. In-cylinder flow characteristics at the time of fuel injection and subsequent interactions with fuel sprays and combustion are the fundamental considerations for the engine performance and exhaust emissions of a diesel engine. Computational fluid dynamics (CFD) is a powerful tool for the computation of fluid flow in complex geometries. The calculation of the flow field in the complex combustion

chamber geometry is a great challenge. With the help of CFD, results can be used for the optimization of the combustion chamber geometry regarding the improvement of efficiency and the reduction of emissions in existing engine and can be used for new developments.

The aim of this work is to study the effect of combustion geometry on air flow and thereby to improve the performance of a four stroke, single cylinder 5.2 kW engine running at 1500 rpm for biodiesel operation. Hence, virtual prototypes of the piston with five different combustion chamber geometries were created and analyzed using CFD software package.

Motivation

The high fuel efficiency of diesel engines has led to their use in many fields including transportation, electrical power generation and agricultural machinery [9, 10]. However, the rapid depletion of fossil fuel with increased environmental concern has increased interest and efforts to produce an alternative to diesel [11]-[14]. Use of biodiesel as an alternative fuel can contribute significantly towards the twin problem of fuel crises and environmental pollution. Researchers [15, 16] have shown that biodiesel fuel exhibits physico-chemical properties which are similar or some even better than to those of diesel and hence can be used in diesel engines. However, certain properties of biodiesel such as viscosity, calorific value, density and volatility differ from diesel.

The high viscosity of biodiesel affects injection characteristics. Although transesterification reduces viscosity of biodiesel [17, 18], the viscosity of biodiesel was found to be 50 to 80% higher than diesel [19]. The poor atomization, insufficient in-cylinder air motion and low volatility of biodiesel lead to difficulty in the air-fuel mixing. Inadequate air-biodiesel mixing and sluggish evaporation process significantly affect the combustion process [20] leading to poor performance of biodiesel fueled diesel engine [21]-[32]. The inferior performance of biodiesel operated diesel engine in comparison with conventional diesel fueled diesel engine is mainly due to change in fuel properties, engine design and operating parameters. In addition in DI diesel engine, the combustion chamber has been optimized for combustion of diesel, including improvement of mixing between injected fuel and in-cylinder air, and not for biodiesel. Apart from injection parameters, the shape of the combustion chamber can also help to form better mixtures. The shape of the combustion chamber and the fluid dynamics inside the chamber are of great importance in biodiesel combustion. As the piston moves upward, the gas is pushed into the piston bowl. The geometry of the piston bowl can be designed to produce a squish and swirling action which can improve the fuel/air mixture before ignition takes place. Therefore to achieve improved performance and further reductions in emissions, rapid

and better air-biodiesel mixing is the most important requirement. Researchers [33] have carried out simulation studies to investigate the effect of piston bowl geometry on both engine performance and combustion efficiency in a direct injection (DI), turbocharged diesel engine for heavy-duty applications using STAR-CD. The simulation results show that, toroidal bowl with lip enhance the turbulence and hence results in better air-fuel mixing. As a result, the indicated specific fuel consumption and soot emission reduced, although the NO_x emission is increased owing to better mixing and a faster combustion process. Prasad et al [34] studied the effect of swirl induced by piston bowl geometries on pollutant emissions from a single cylinder diesel engine using CFD. Pollutant emission measurements indicated a reduction in emissions for toroidal, with slightly re-entrant type combustion chamber due to improved air swirl.

As the combustion chamber geometry affects the air-fuel mixing and the subsequent combustion and pollutant formation processes in a DI diesel engine an attempt has been made here to investigate the effect of combustion chamber design on air motion and thereby air-biodiesel mixing. In this investigation, numerical simulation was carried out using five types of combustion chamber geometries to analyze the air motion.

Geometric Modelling

The engine studied in this work was a stationary, single-cylinder, DI diesel engine with five different piston bowl shapes. These shapes are representative of the geometries usually employed for the optimum combustion process in real engines. The piston named HCC had a Hemispherical Combustion Chamber and used as a baseline model. Two pistons having open combustion geometries namely Shallow depth Combustion Chamber and Toroidal Combustion Chamber (named SCC and TCC respectively) and two other pistons having re-entrant combustion chamber geometries namely Shallow depth Re-entrant Combustion Chamber and Toroidal Re-entrant Combustion Chamber (named SRCC and TRCC respectively) were used. In order to maintain the compression ratio of the engine under consideration, while modeling, the bowl volumes for all the combustion chamber configurations were kept constant. Figure 1 shows the shapes and dimensions of five combustion chamber geometries used. The inlet valve axis is offset from the cylinder axis by 18.5 mm in the x direction and 2.0 mm in the y direction. The standard specification of the base engine selected for the simulation is given in Table 1.

Table 1: Standard engine specifications

| Make | Kirloskar TV1 |
|--------------------|----------------------------------------------------------------|
| Type | Vertical diesel engine, 4stroke, water cooled, single cylinder |
| Displacement | 661 cc |
| Bore & Stroke | 87.5 mm & 110 mm |
| Compression ratio | 17.5:1 |
| Fuel | Diesel |
| Rated brake power | 5.2 kW @ 1500 rpm |
| Ignition system | Compression ignition |
| Combustion chamber | Hemispherical combustion chamber |

Modelling Methodology

The modeling and analysis of the combustion chamber configurations have been carried out using software packages. The software packages GAMBIT and STAR-CD were used. The pre-processor GAMBIT was used to create the computational domain of the engine and computational fluid dynamics code STAR-CD was used for solution of governing equations and post processing the results [35, 36]. A hexahedral block structured mesh was employed for the entire computational domain of the engine. Figure 2 shows the computational meshes employed for the simulation of different combustion chamber geometries.

Flow conditions inside the cylinder were predicted by solving momentum, continuity and energy equations [37, 38]. The simulation was carried out for a constant engine speed at non-reacting condition. Constant pressure boundary conditions were assigned for both intake and exhaust ports, so the dynamic effects were neglected. The initial values for pressure and temperature were 1.02 bar and 303 K respectively, with both variables considered as homogeneous in the whole domain. As the residual swirl of the flow in the cylinder at the end of the exhaust stroke was not taken into account, the flow was supposed to be quiescent initially. The initial turbulence intensity was set at 5% of the mean flow, and the integral length scale was estimated with the mixing length model of Prandtl [39]. The walls of the intake ports, the lateral walls of the valves and the cylinder head, the cylinder wall and the piston crown that form the walls of the combustion chamber were considered adiabatic.

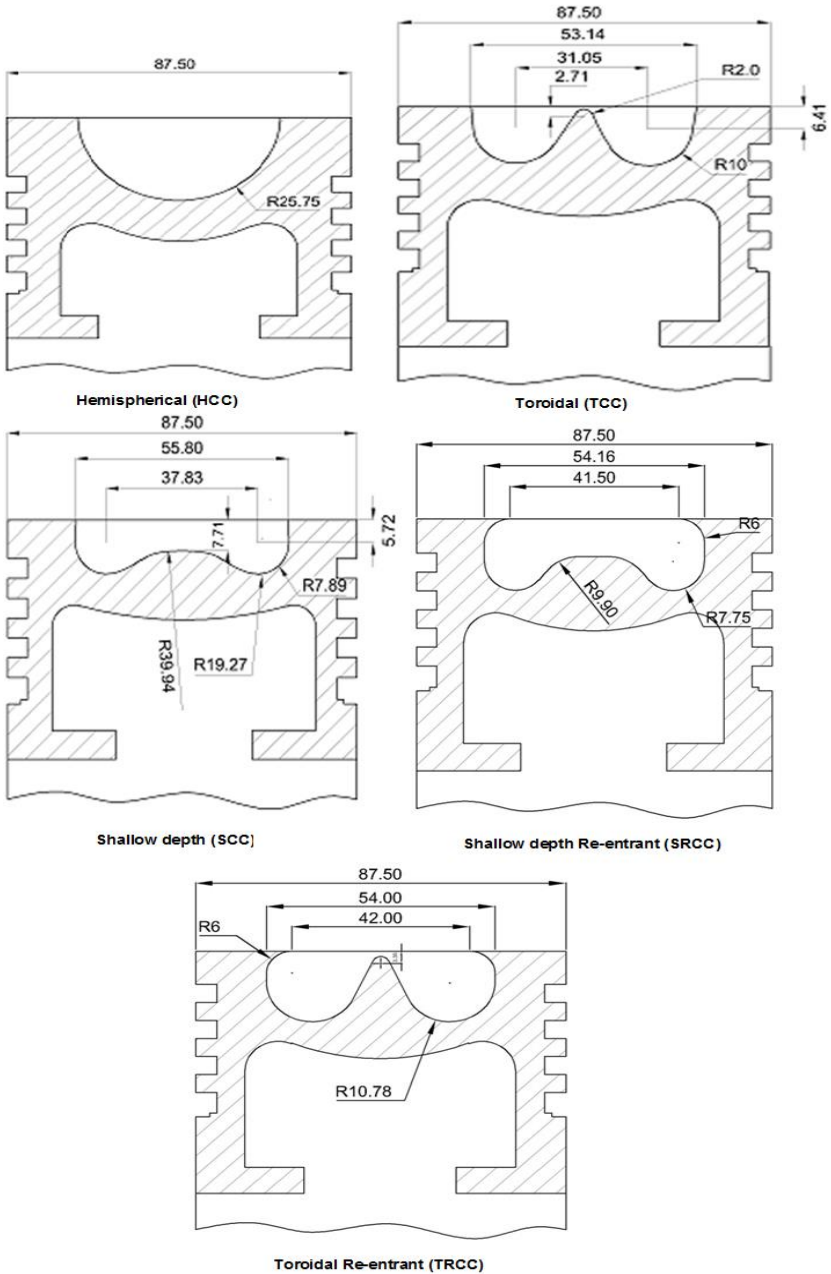


Figure 1: Schematic diagram of combustion chambers employed

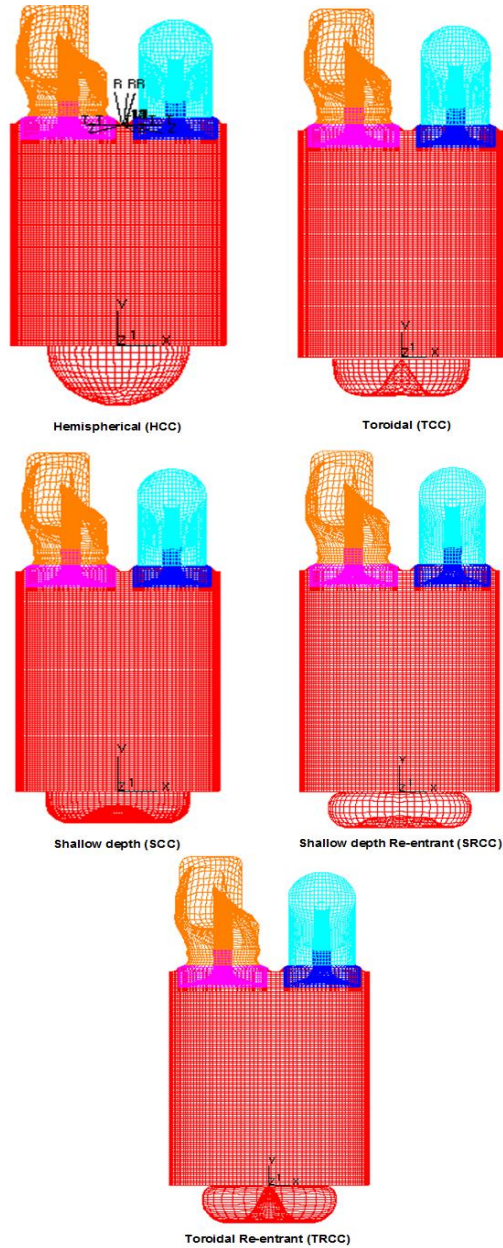


Figure 2: Computational domains of different combustion chamber geometries

The calculations began at TDC of the intake stroke and completed at 30 degrees after TDC (aTDC) of compression. In order to study the fluid flow behaviour in the analysis, quantities such as swirl velocity, Turbulent Kinetic Energy (TKE) and Swirl-Ratio (SR) were computed for the in-cylinder flow field about the cylinder axis. The quantity known as Swirl ratio is expressed as [3, 40],

$$SR = \frac{60H_z}{2\pi M_z \Omega_{cs}}$$

Where, H_z represents the total angular momentum of the in-cylinder fluid about the cylinder axis, M_z is the total moment of inertia of the fluid about the cylinder axis, Ω_{cs} is the angular speed of the crankshaft in rpm.

Results and Discussion

A numerical simulation study was carried out to investigate the effect of combustion chamber configuration on air motion inside the cylinder of a DI diesel engine motored at 1500 rpm. Five combustion chamber configurations namely HCC, SCC, TCC, SRCC and TRCC were modeled for the flow analysis in the first stage. This section describes the results from a comprehensive CFD study on the flow characteristics inside the cylinder of the engine. The flow in the cylinder during the intake and compression stroke was analyzed, and presented in the following section.

Swirl velocity

Figure 3 to 7 show the swirl velocity for the different combustion chamber geometries at compression TDC. The predicted swirl velocity was low for the open bowl configurations compared to the re-entrant bowl configurations. TRCC showed higher swirl mean velocity component than other combustion chamber geometries in all the locations. It was due to the induced tangential component of TRCC, which was able to sustain until the end of compression. The intensity of maximum swirl velocity at the end of compression stroke for TRCC (Max: 18.95 m/s) was observed maximum and a strong recirculation was observed due to the combustion chamber geometry. This will help in better fuel air interaction, which will lead to better combustion and performance. In the case of SCC swirl velocity was very low (Max: 7.743 m/s) and for HCC (Max: 10.56 m/s) and TCC (Max: 12.28 m/s) swirl velocity was higher than SCC. The maximum swirl velocity of SRCC (Max: 14.02 m/s) lie in between TCC and TRCC.

It was observed that for all the combustion chamber geometries, the radial distribution of swirl velocity component increased as the observation

location was moved towards the bowl from the cylinder wall. When the observation location moved towards the bowl the frictional effect was less than the location of the cylinder wall [41, 42]. This led to the increase of mean swirl velocity near the bowl. Same trend was observed for all other combustion chamber configurations. It can also be seen from the Figures 3, 5, 6 and 7 that the swirl velocity was not so uniform throughout the cylinder and maximum occurred near the outer periphery of the bowl. However for SCC (Figure 4), the flow structure was so uniform and the maximum velocity magnitude was considerably less compared to TRCC. The TRCC created a strong swirl velocity at all locations due to its configuration. At compression TDC the max swirl velocity for HCC, SCC, TCC and SRCC were lower by 44%, 59%, 35.2% and 26% respectively compared to TRCC. The calculated velocities were generally in good agreement with the experimental results of Chen et al [43].

Swirl ratio

Figure 8 shows the details of swirl ratio (SR) during suction and compression for all the combustion chamber geometry configurations viz., HCC, SCC, TCC, SRCC and TRCC. As could be seen from the Figure 8 that, during compression the SCC produced very low swirl with peak swirl ratio value of 2.17, whereas, the TRCC produced the maximum swirl with peak swirl ratio value around 3.26, which was 1.5 times higher than SCC. The SRCC had swirl ratio in between TRCC and TCC with peak swirl ratio value around 3.04. It was also seen that increase of swirl ratio was more or less same for all the combustion chambers during the early stage of suction process.

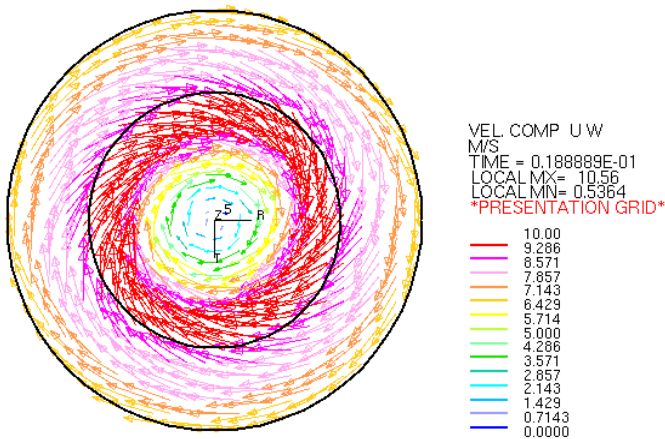


Figure 3: Swirl velocity vector at 360° CA aTDC for HCC

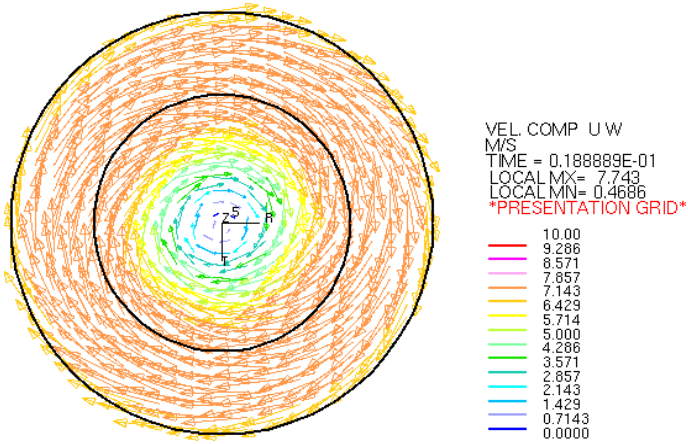


Figure 4: Swirl velocity vector at 360° CA aTDC for SCC

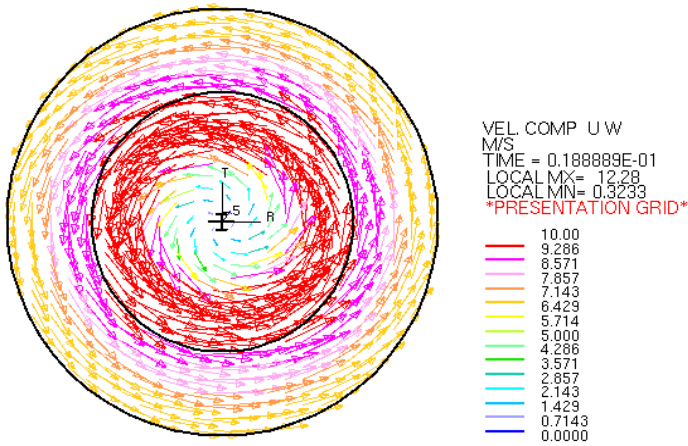


Figure 5: Swirl velocity vector at 360° CA aTDC for TCC

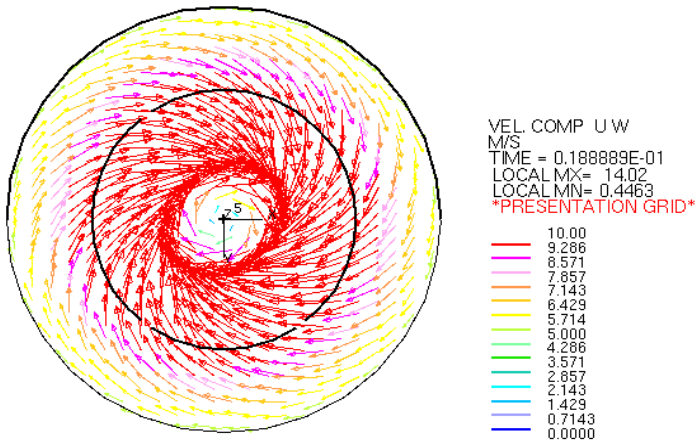


Figure 6: Swirl velocity vector at 360° CA aTDC for SRCC

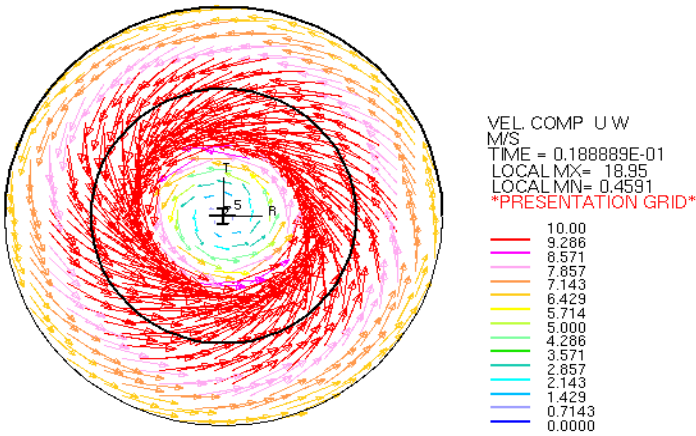


Figure 7: Swirl velocity vector at 360° CA aTDC for TRCC

This shows that combustion chamber plays a less significant role on swirl during suction process. During the early stage of suction process, the increase in swirl between 0° and 110° aTDC was quite considerable [44]. Further, it may be noted that the first peak occurring around 110° aTDC from the start of suction. This was attributable to the piston acceleration and reduction of pressure inside the cylinder. After reaching the peak around 110° aTDC,

swirl ratio started reducing due to the increase in volume of cylinder and closing of the intake valve. This was also caused by the reduction of mass flow rate of incoming air and the friction between the wall and air inside the cylinder.

This decreasing trend continued in the first part of the compression stroke due to friction at the wall. However, beyond 300° aTDC swirl ratio started increasing. This was due to the axial upward flow induced a gradual increase of the swirl velocity in the top part of the piston [45]. It was also noted that the increase in swirl was quite small for SCC and the maximum swirl ratio was obtained for TRCC. Figure 8 shows the high intensity of swirl ratio for the TRCC, due to the combustion chamber configuration. Thus, it was well established that TRCC configuration was the best for sustaining swirl near the compression TDC. This result was in good agreement with the findings of Gunabalan and Ramaprabhu [41]. The different combustion chamber configurations i.e. HCC, SCC, TCC and SRCC had lower maximum swirl ratio by 22%, 33%, 14% and 6.7% respectively at 360° CA aTDC compared to that of TRCC. The maximum swirl ratio obtained for five combustion chamber geometries are tabulated in Table 2. The predicted swirl ratio values were largely in good conformity with the calculated swirl ratio results of Payri et al [46].

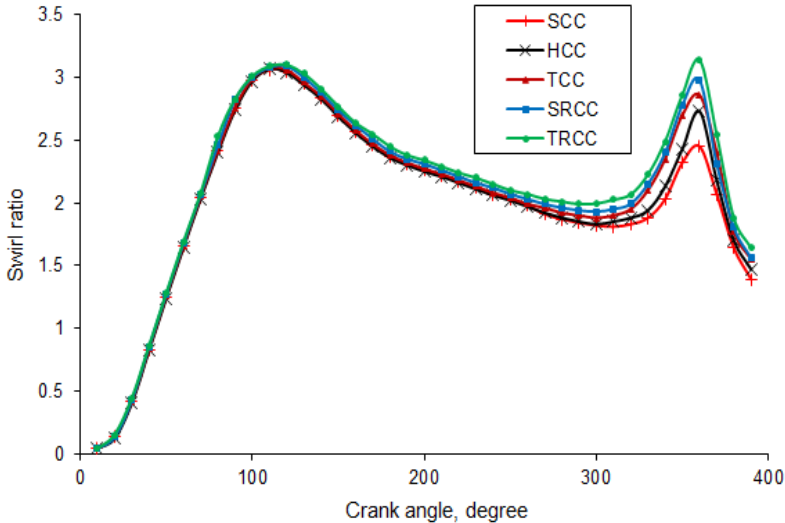


Figure 8 Comparison of swirl ratio for different combustion chambers

From Table 2 it was observed that, TRCC showed higher swirl ratio of 28% than baseline bowl HCC. These predictions were similar to the findings of

Payri et al [46], Gunabalan and Ramaprabhu [41] and B. Paul and V. Ganesan [44]. The projection at the center of the TRCC and the lip provided reduced the effective diameter of the chamber, thereby increased the angular momentum which results in higher swirl ratio. After compression TDC, during the expansion stroke, reverse squish as the flow exits from the piston bowl and wall friction contribute to the sudden fall of the swirl velocity.

Table 2: Mass average swirl ratio for five different combustion chamber geometries

| Combustion chamber geometry | Max swirl during suction stroke | Max swirl during compression stroke |
|-----------------------------|---------------------------------|-------------------------------------|
| HCC | 3.07 | 2.52 |
| SCC | 3.06 | 2.17 |
| TCC | 3.08 | 2.79 |
| SRCC | 3.12 | 3.04 |
| TRCC | 3.16 | 3.26 |

Turbulent kinetic energy

Figure 9 to Figure 13 show the Turbulent Kinetic Energy (TKE) for different configurations of combustion chambers at compression TDC. It was observed that the configuration of the combustion chamber of the engine directly affects the turbulence of the fluid inside the cylinder particularly during the end of the compression stroke. During the compression process the highest value of TKE was observed for TRCC at TDC [34]. At the beginning of suction stroke the air flows smoothly into the cylinder and the TKE gradually increased from 0° CA to maximum valve lift (at 110° crank angle) and then decreased with respect to the piston movement [47]. This was due to the mass flow reduction caused by the closing of the valve. It was also observed that high values of turbulent kinetic energy were found at the inlet valve exit, for all configurations. Turbulent kinetic energy started to decrease when the valve lift reached higher level and declined during the second half of induction [44]. Further, similar type of variation in TKE was reported by B. Murali Krishna and J.M. Mallikarjuna [48].

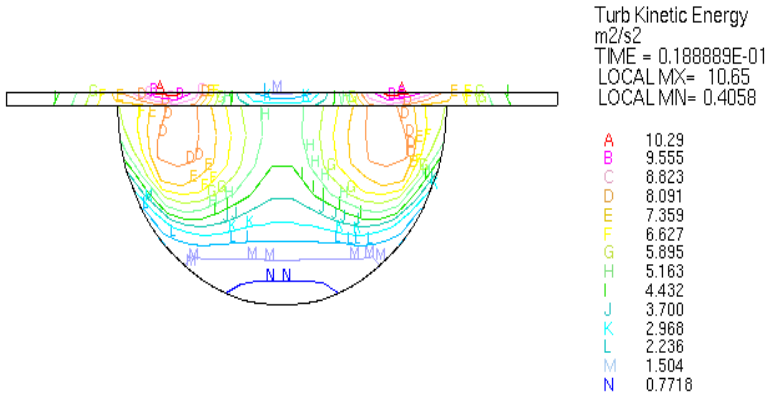


Figure 9: TKE contour plot for HCC at 360° CA aTDC

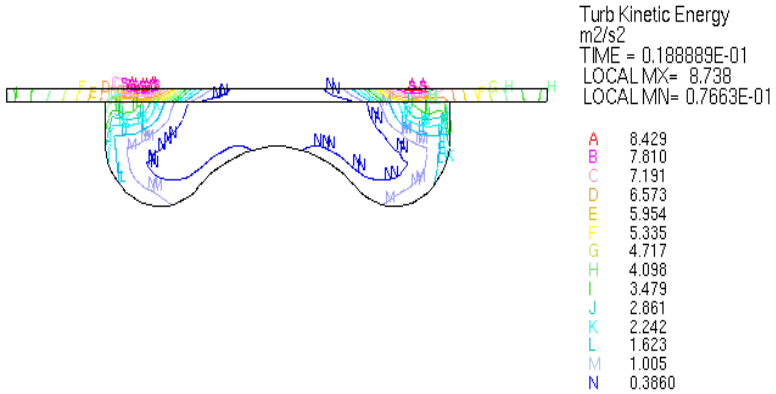


Figure 10: TKE contour plot for SCC at 360° CA aTDC

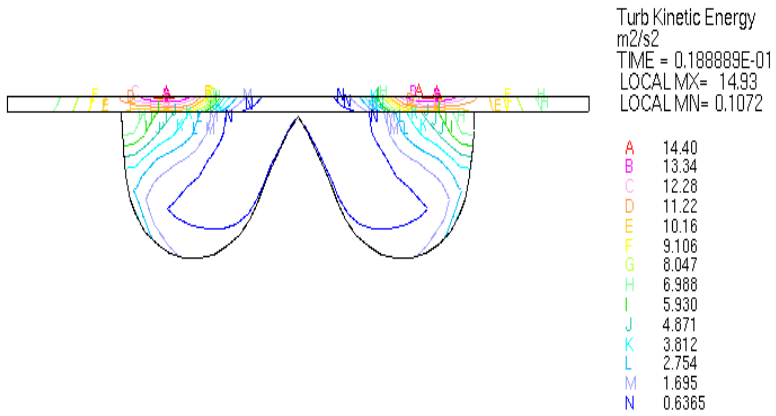


Figure 11: TKE contour plot for TCC at 360° CA aTDC

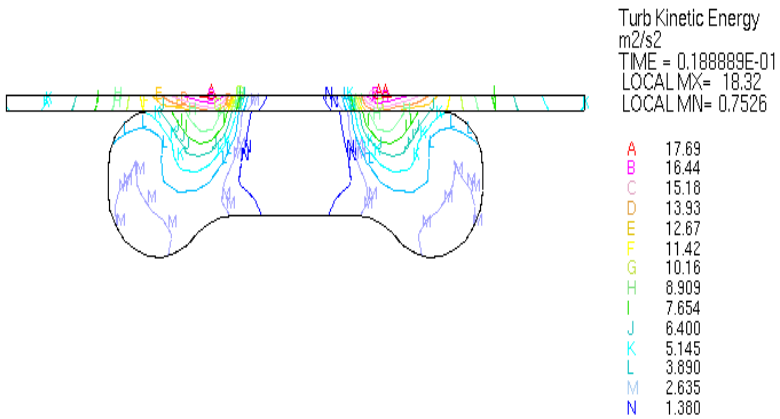


Figure 12: TKE contour plot for SRCC at 360° CA aTDC

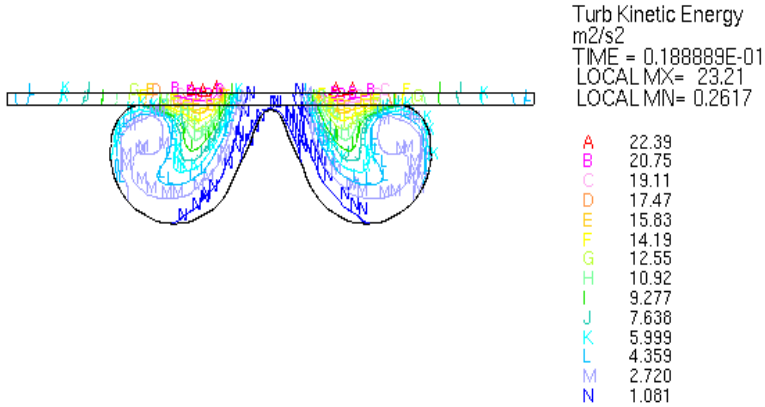


Figure 13: TKE contour plot for TRCC at 360° CA aTDC

For all the five combustion chamber geometries the same trend was observed during induction process and the variation of TKE for all five combustion chambers were identical; this means that the combustion chamber geometry does not play any major role in the turbulence generation during induction [46]. However, it was observed that during compression, the combustion chamber plays an important role in generating the turbulence inside the cylinder.

As could be seen from the Figure 14 that, at the end of compression, the TRCC produced very high turbulence with peak TKE value of around $23.21 \text{ m}^2/s^2$ whereas the baseline HCC produced the peak TKE value of around $10.65 \text{ m}^2/s^2$, which was 2.18 times lower than TRCC. The SRCC had peak TKE value of around $18.32 \text{ m}^2/s^2$ which, lie in between TRCC and TCC. It was also noted that the peak TKE value, was quite small for SCC ($8.74 \text{ m}^2/s^2$) compared to other combustion chamber configurations. The peak TKE values for SRCC, TCC, SCC and HCC in comparison with that of TRCC decreased by 21%, 35.7%, 54% and 62% respectively at 360° CA aTDC. From the Figure 14 it can also be seen that lower values of TKE were observed for open bowl than re-entrant chambers, since the squish effect in these combustion chambers was smaller. The turbulent kinetic energy for the TRCC was found higher at compression TDC and early stage of expansion stroke. This was attributable to the shape of the combustion chamber i.e. the projection at the center of the TRCC and the lip provided reduced the effective diameter of the chamber, which results in higher TKE [45]. Thus TRCC seem to conserve better their turbulent energy.

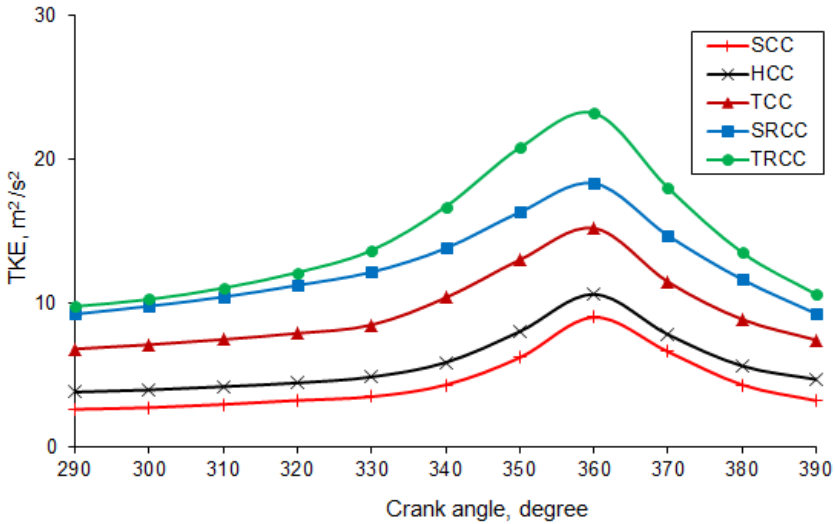


Figure 14: In-cylinder peak TKE at the end of compression for different combustion chambers

Conclusion

Based on the simulation of non-firing, in-cylinder flow analysis for the five combustion chamber configurations of DI diesel engine, the following observations and results can be highlighted;

1. Swirl generation of TRCC configuration was better than other piston bowl configurations. The effect of bowl geometry was quite prominent during the compression than the induction process. The predicted swirl velocity was low for the open bowl configurations compared to other two re-entrant bowl configurations.
2. It was found that piston bowl plays a less significant role on swirl generation during suction process. During compression the TRCC produced the maximum swirl with peak swirl ratio value of around 3.26, which was 1.29 times higher than the baseline HCC. Compared to TRCC, the other piston bowl configurations i.e. HCC, SCC, TCC and SRCC had lower, maximum swirl ratio by 22%, 33%, 14% and 6.7% respectively at 360° CA aTDC.
3. TRCC configuration was found to have higher in-cylinder turbulence compared to the other piston bowl configurations. The peak TKE values for SRCC, TCC, SCC and HCC in comparison with that of TRCC were

lower by 21%, 35.7%, 54% and 62% respectively at 360° CA aTDC. Comparison of TKE shows that, the configuration of the combustion chamber directly affects the turbulence of the fluid inside the cylinder, particularly at the end of the compression stroke.

The results of these investigations show that during compression of DI diesel engine, the combustion chamber configuration plays a significant role in deciding the swirl and turbulence levels inside the cylinder. TRCC provides better air motion in the cylinder than other combustion chamber geometries.

References

- [1] B. Challen and R. Barnescu, Diesel Engine Reference Book, Society of Automotive Engineers, (Bath Press, England, 1999).
- [2] V. Ganesan, Internal Combustion Engines, 2nd Edn. (Tata McGraw Hill Publishers, New Delhi, 1998), pp. 295–355.
- [3] J. B. Heywood, Internal Combustion Engine fundamentals, (McGraw Hill Publications, New York, 1988), pp.682–692.
- [4] F. Brandl, Reverencic, W. Cartellieri and J.C. Dent, “Turbulent air flow in the combustion bowl of a DI diesel engine and its effect on engine performance,” SAE Paper 790040 (1979).
- [5] A.D. Risi, T. Donateo, D. Laforgia, "Optimization of the Combustion Chamber of Direct Injection Diesel Engines" SAE 2003-01-1064 (2003).
- [6] D.A. Kouremenos, D.T. Hountalas, A.D. Kouremenos. “Experimental investigation of the effect of fuel composition on the formation of pollutants in direct injection diesel engines,” SAE paper 1999-01-0189 (1999).
- [7] H. Schapertons, F. Thiele, "Three dimensional computations for flow fields in DI piston bowls". SAE 860463, (1986).
- [8] F.E. Corcione, A. Fusca and G. Valentino, "Numerical and Experimental Analysis of Diesel Air Fuel Mixing" SAE 931948 (1993).
- [9] M.N. Nabi, M. S. Akhter and M.M.Z. Shahadat, “Improvement of engine emissions with conventional diesel fuel and diesel–biodiesel blends,” Bioresource Technology 97, 372–378 (2006).
- [10] Chotwichien, A. Luengnaruemitchai and S. Jai-In, “Utilization of palm oil alkyl esters as an additive in ethanol–diesel and butanol–diesel blends,” Fuel 88(9), 1618-1624 (2009).
- [11] M.M. Hasan, M.M. Rahman, and K. Kadirgama, “A review on homogeneous charge compression ignition engine performance using biodiesel–diesel blend as a fuel”, International Journal of Automotive and Mechanical Engineering 11, 2199-2211 (2015).

- [12] A.S. Ramadhas, S. Jayaraj and C. Muraleedharan, "Use of vegetable oils as I.C. engine fuel- a review". *Renewable Energy*, 29(5), 727-742 (2004).
- [13] S.C. Bhupendra, K. Naveen and M.C. Haeng, "A study on the performance and emission of a diesel engine fueled with jatropha biodiesel oil and its blends", *Energy*, 37, 616–622 (2012).
- [14] S. Kumar, A. Chaube and S.K. Jain, "Experimental investigation of C.I. engine performance using diesel blended with jatropha biodiesel", *International Journal of Energy and Environment*, 3(3):471-484 (2012).
- [15] P.K. Sahoo and L.M. Das, "Combustion analysis of jatropha, karanja and polanga based biodiesel as fuel in a diesel engine", *Fuel*, 88(6), 994–999 (2009).
- [16] C.E. Goering, A.W. Schwab, M.J. Daugherty, E.H. Pryde and A.J. Heakin, "Fuel properties of eleven vegetable oils", *Transactions of ASAE*, 25(6), 1472-1477 (1982).
- [17] B. Baiju, M.K. Naik and L.M. Das, "A comparative evaluation of compression ignition engine characteristics using methyl and ethyl esters of Karanja oil," *Renewable Energy* 34(6), 1616-1621 (2009).
- [18] P.K. Devan and N.V. Mahalakshmi, "Study of the performance, emission and combustion characteristics of a diesel engine using poon oil-based fuels," *Fuel Processing Technology* 90(4), 513-519 (2009).
- [19] M. Lapuerta, O. Armas and J.R. Fernandez, "Effect of biodiesel fuels on diesel engine emissions," *Progress in Energy and Combustion Science* 34, 198–223 (2008).
- [20] J.M. Desantes, J. Arregle, S. Ruiz and A. Delage, "Characterization of the injection combustion process in a di diesel engine running with rape oil methyl ester", *SAE paper 1999-01-1497* (1999).
- [21] K.K. Radha, S.N. Sarada, K. Rajagopal and E.L. Nagesh, "Performance and emission characteristics of CI engine operated on vegetable oils as alternate fuels", *International Journal of Automotive and Mechanical Engineering*, 4, 414-427 (2011).
- [22] P.K. Sahoo, S.N. Naik and L.M. Das, "Studies on biodiesel production technology from jatropha curcas and its performance in a CI engine", *J. Agri. Eng. Indian. Soc. Agri. Eng. (ISAE)*, 42(2), 18–24 (2005).
- [23] B. Gokalp, E. Buyukkaya and H.S. Soyhan, "Performance and emissions of a diesel tractor engine fueled with marine diesel and soybean methyl ester", *Biomass and Bioenergy*, 35(8), 3575-3583 (2011).
- [24] Z. Lei, C.S. Cheung, W.G. Zhang and H. Zhen, "Combustion, performance and emission characteristics of a DI diesel engine fueled with ethanol–biodiesel blends", *Fuel*, 90(5), 1743-1750 (2011).
- [25] D.R. Constantine, M.D. Athanasios, G.G. Evangelos and C.R. Dimitrios, "Investigating the emissions during acceleration of a

- turbocharged diesel engine operating with bio-diesel or n-butanol diesel fuel blends”, *Energy*, 35(12), 5173-5184 (2010).
- [26] S. Puhan, N. Vedaraman, G. Sankaranarayanan and B.V.B. Ram, “Performance and emission study of mahua oil (*madhuca indica* oil) ethyl ester in a 4-stroke natural aspirated direct injection diesel engine”, *Renewable Energy*, 30, 1269–1278 (2005).
- [27] T. Pi-qiang, H. Zhi-yuan, L. Di-ming and L. Zhi-jun, “Exhaust emissions from a light-duty diesel engine with *jatropha* biodiesel fuel”, *Energy*, 39(1) 356-362 (2012).
- [28] B. Vicente, M.L. Jose, P. Benjamin and G.L. Waldemar, “Comparative study of regulated and unregulated gaseous emissions during NEDC in a light-duty diesel engine fuelled with Fischer (2011).
- [29] S. Saravanan , G. Nagarajan , R.G. Lakshmi Narayana and S. Sampath, “Combustion characteristics of a stationary diesel engine fuelled with a blend of crude rice bran oil methyl ester and diesel”, *Energy*, 35(1), 94-100 (2010).
- [30] Ekrem Buyukkaya, “Effects of biodiesel on a DI diesel engine performance, emission and combustion characteristics” *Fuel*, 89(10), 3099-3105 (2010).
- [31] H. Song, B.T. Tompkins, J.A. Bittle and T.J. Jacobs, “Comparisons of NO emissions and soot concentrations from biodiesel-fuelled diesel engine”, *Fuel*, 96, 446-453 (2012).
- [32] A.K. Agarwal, “Biofuels (alcohols and biodiesel) applications as fuels for internal combustion engines” *Prog. Energy Combust. Sci*, 33, 233-271 (2007).
- [33] S. P. Venkateswaran and G. Nagarajan, “Effects of the re-entrant bowl geometry on a DI turbocharged diesel engine performance and emissions - a CFD approach”, *J Eng Gas Turb Power*, 132(12), 122803-13 (2010).
- [34] B.V.V.S.U. Prasad, C.S. Sharma, T.N.C. Anand and R.V. Ravikrishna, “High swirl-inducing piston bowls in small diesel engines for emission reduction”, *Applied Energy*, 88(7), 2355–2367 (2011).
- [35] M. Auriemma, F.E. Corcione, R. Macchioni and G. Valentino, “Interpretation of air motion in reentrant bowl in-piston engine by estimating Reynolds stresses”, *SAE Paper No. 980482* (1998).
- [36] T. Okazaki, H. Miyazaki, M. Sugimoto, S. Yamada and M. Aketa, “CFD approach for optimum design of DI combustion system in small versatile diesel engine”, *SAE Paper No. 1999-01-3261* (1999).
- [37] Z.U.A. Warsi, “Conservation form of the Navier-Stokes equations in general nonsteady coordinates”, *AIAA Journal*, 19(2), 240-242 (1981).
- [38] S.C. Kong, Z. Han, and R.D. Reitz, “The development and application of a diesel ignition and combustion model for multidimensional engine simulation”, *SAE Paper No. 950278* (1995).

- [39] B.E. Launder and D.B. Spalding, Lectures in mathematical models of turbulence, (Academic Press Inc, London, 1972).
- [40] Y. Shi, H.W. Ge and R.D. Reitz, Computational optimization of internal combustion engines, (Springer, London, 2011), pp.151–152.
- [41] Gunabalan and R. Ramaprabhu, “Effect of piston bowl geometry on flow, combustion and emission in DI diesel engine--a CFD approach”, *International Journal of Applied Engineering Research*, 4(11), 2181-2188 (2009).
- [42] Jayashankara and V. Ganesan, “Effect of fuel injection timing and intake pressure on the performance of a DI diesel engine-A parametric study using CFD”, *Energy Conversion and Management*, 51(10), 1835-1848 (2010).
- [43] Chen, A. Veshagh and S. Wallace, “Intake flow predictions of a transparent DI diesel engine”, SAE Paper No. 981020 (1998).
- [44] Paul and V. Ganesan, “Flow field development in a direct injection diesel engine with different manifolds”, *International Journal of Engineering, Science and Technology*, 2(1), 80-91 (2010).
- [45] P. Vijayakumaran, R.Elajaraja, A. Muthuvel, Dr. M.Subramanian and R. Murukesan, “ Numerical simulation of combustion chamber geometry on a H.S.D.I. diesel engine – a CFD approach”, *IOSR Journal of Mechanical and Civil Engineering*, 4, 66-73 (2014).
- [46] F. Payri, J. Benajes, X. Margot and A. Gil, “CFD modeling of the in-cylinder flow in direct-injection diesel engines”, *Computers & Fluids*, 33, 995–1021 (2004).
- [47] B.M. Krishna and J.M. Mallikarjuna, “Characterization of flow through the intake valve of a single cylinder engine using particle image velocimetry”, *Journal of Applied Fluid Mechanics*, 3(2), 23-32 (2010).
- [48] B.M. Krishna and J.M. Mallikarjuna, “Effect of engine speed on in-cylinder tumble flows in a motored internal combustion engine - an experimental investigation using particle image velocimetry”, *Journal of Applied Fluid Mechanics*, 4(1), 1-14 (2011).